ing the distance between two charge groups: the conjugate acid and its specific counter anion. This is equivalent to a 1:1 electrolyte. However, it must be remembered that the protein, by virtue of its ionic groups, is itself a polyelectrolyte. This electrically neutral molecule contains a large number of positive and negative centers, and instead of analyzing the charge state as a 1:1 electrolyte, it should be analyzed as a polyelectrolyte. For this purpose, the positive charge of the conjugate acid can be visualized to be located at some fixed point in the electrostatic field. With respect to the conjugate acid the electrostatic field will have one excess negative charge. In comparison to the order in a crystal of an ionic compound, the protein may be considered as a random matrix of fixed charges. The center of negative charge density with respect to the conjugate acid will be a contribution of the nearest negative groups, and this negative charge density does not have to be located at the same point as the negative group. The distance from the cation to the center of negative charge density of the electrostatic field is equal to the $r_c + r_a$ term. This means that with respect to the conjugate acid each protein conformation will have a certain center of negative charge density, and consequently, the resulting change in electrostatic interaction energy will induce a change in excitation energy.

References

Akhtar, M., Blosse, P. T., and Dewhurst, P. B. (1967), *Chem. Commun.*, 631.

Audrieth, L. F., and Kleinberg, J. (1953), *in* Non-aqueous Solvents, New York, N. Y., Wiley, p 156.

Blatz, P. E., Baumgartner, N., Balasubramaniyan, P., Balasubramaniyan, V., and Stedman, E. (1971a), *Photochem. Photobiol. 14*, 531.

Blatz, P. E., Baumgartner, N., and Dewhurst, S. (1968a), *J. Phys. Chem. 72*, 2960.

Blatz, P. E., Johnson, R. H., Mohler, J. H., Al-Dilaimi, S. K., Dewhurst, S., and Erickson, J. O. (1971b), *Photochem. Photobiol. 13*, 237.

Blatz, P. E., and Mohler, J. H. (1970), *Chem. Commun.*, 614.

Blatz, P. E., and Pippert, D. L. (1966), *Tetrahedron Lett.*, 1117.

Blatz, P. E., and Pippert, D. L. (1968), *J. Amer. Chem. Soc. 90*, 1296.

Blatz, P. E., Pippert, D. L., and Balasubramaniyan, V. (1968b), *Photochem. Photobiol. 8*, 309.

Bownds, D. (1967), *Nature (London) 216*, 1178.

Braude, E. A. and Waight, E. S.(1954), *Progr. Stereochem. 1*, 142.

Brown, R. D., and Penfold, A. (1957), *Trans. Faraday Soc. 53*, 397.

Erickson, J. O., and Blatz, P. E. (1968), *Vision Res. 8*, 1367.

Kimbel, R. L., Poincelot, R. P., and Abrahamson, E. W. (1970), *Biochemistry 9*, 1817.

Malhotra, S. S., and Whiting, M. C. (1960), *J. Chem. Soc.*, 3812.

Nesbet, R. K. (1955), *Proc. Roy. Soc., Ser. A 230*, 312.

Pauling, L. (1960), *in* The Nature of the Chemical Bond, 3rd ed, Ithaca, N. Y., Cornell University Press, p 514.

Pitt, G. A. J., Collins, F. D., Morton, R. A., and Stok, P. (1955), *Biochem. J. 59*, 122.

Roothaan, C. C. J. (1951), *Rev. Mod. Phys. 23*, 69.

Weisberger, A., Prosbauer, E., and Troops, E. (1955), *in* Organic Solvents, New York, N. Y., Interscience.

Mössbauer Parameters of Putidaredoxin and Its Selenium Analog†

E. Münck, P. G. Debrunner,* J. C. M. Tsibris,‡ and I. C. Gunsalus

ABSTRACT: Mössbauer spectra of ^{57}Fe-enriched putidaredoxin, a 2Fe–2S protein from *Pseudomonas putida*, and of its selenium analog were measured. The data were analyzed with the help of computer programs that calculate Mössbauer spectra for given sets of magnetic and electric hyperfine interaction tensors. With the g tensor and some values of the magnetic hyperfine tensors known from electron spin resonance and electron nuclear double resonance data we were able to find parameters that reproduce the data quite well. The parameters found for the two irons in the reduced, paramagnetic protein are typical of high-spin ferric, $S_a = 5/2$, and ferrous iron, $S_b = 2$, respectively. Spectra measured in strong magnetic fields show conclusively that the spins residing on each individual iron couple antiferromagnetically to a total spin of $S = 1/2$. The magnetic hyperfine tensor of the ferric iron is relatively small and highly anisotropic which implies strong covalency and relatively low symmetry in the arrangement of the ligands. The parameters of the ferrous iron are compatible with distorted tetrahedral symmetry of the ligands. The two iron atoms in the oxidized, diamagnetic protein are interpreted as high-spin ferric, $S = 5/2$, coupled to a total spin of zero.

Putidaredoxin is an iron–sulfur protein of molecular weight 12500 isolated from *Pseudomonas putida* (Cushman *et al.*, 1967). It acts as a specific one-electron transfer agent in a multienzyme system that hydroxylates camphor (Gunsalus, 1968). Each molecule contains two iron and two acid-labile sulfur atoms that can be replaced by isotopically enriched iron and sulfur or selenium, respectively (Tsibris *et al.*,

† From the Department of Physics and Department of Biochemistry, University of Illinois at Urbana-Champaign, Urbana, Illinois 61801. *Received October 8, 1971.* Supported in part by grants from the U. S. Public Health Service (GM 16406 and AM 00562) and by Research Career Development Award K4-AM-42368 (J. C. M. T.).

‡ Present address: Department of Biochemistry, University of Florida, Gainesville, Fla. 32601.

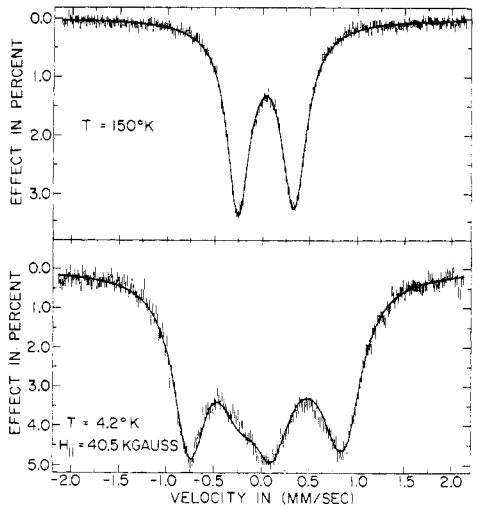

FIGURE 1: Mössbauer spectra of oxidized putidaredoxin in zero field (upper curve) and in a magnetic field of 40.5 kG parallel to the direction of the γ rays observed (lower curve). The solid lines are the results of least-squares fits to the data with the parameters listed in Table I. The zero-field spectrum taken at 150°K was fitted with two Lorentzians of equal areas.[1] The curves in Figures 1–5 are computer generated with a Calcomp plotter. The velocity scales are relative to a ^{57}Co source diffused into copper.

1968a,b). It undergoes a one-electron reduction (Tsibris *et al.*, 1968a), changing from an oxidized, diamagnetic state to a reduced state of spin $S = 1/2$ (Moleski *et al.*, 1970) with a characteristic electron paramagnetic resonance (epr) signal at $g_{\perp} = 1.94, g_{||} = 2.01$ (Der Vartanian *et al.*, 1968). Epr measurements on isotopically enriched proteins have shown that the unpaired spin interacts with the two iron and the labile sulfur or selenium nuclei and with organic sulfur as well (Tsibris *et al.*, 1968a; Orme-Johnson *et al.*, 1968). Thus the redox center comprises the 2Fe–2S complex (Tsibris and Woody, 1970), organic sulfur, and possibly other ligands.

In most of its physical properties putidaredoxin resembles adrenodoxin (Orme-Johnson *et al.*, 1968), an electron carrier in a steroid hydroxylase, and, to a lesser extent, the green plant ferredoxins (Palmer and Sands, 1966). All these 2Fe–2S proteins have similar optical (Cushman *et al.*, 1967; Palmer *et al.*, 1967), epr (Der Vartanian *et al.*, 1967; Orme-Johnson *et al.*, 1968; Palmer and Sands, 1966), endor (Fritz *et al.*, 1971), and Mössbauer spectra (Dunham *et al.*, 1971; Johnson and Hall, 1968) and, since the common features are due to the iron–sulfur complex, the structure of the complex appears to be essentially the same in all of them (Hall and Evans, 1969; Tsibris and Woody, 1970). So far it has not been possible to determine the structure of any of the 2Fe–2S proteins by X-ray diffraction; however, related 1-Fe (Herriott *et al.*, 1970) and 4Fe–4S proteins (Kraut *et al.*, 1968), respectively, have been analyzed by this method.

A number of models have been proposed for the hypothetical structure of the 2Fe–2S complex (Brintzinger *et al.*, 1966; Gibson *et al.*, 1966; Johnson *et al.*, 1969), the most attractive one being that of Gibson *et al.* According to this model, the complex contains an antiferromagnetically coupled pair of iron ions which are both ferric in the oxidized protein, while they are ferrous and ferric, respectively, in the reduced protein. To account for the unusual g values, Gibson *et al.* further assumed that the ligand field of the ferrous ion has distorted tetrahedral symmetry.

The purpose of this communication is to present systematic Mössbauer studies on both putidaredoxin and its selenium analog, Se-putidaredoxin. We have been able to quantitatively interpret the spectra in terms of physical parameters and can compare our results to model predictions. The analysis shows that the reduced protein indeed contains an antiferromagnetically coupled pair of high-spin ferric and ferrous irons; moreover the data are compatible with a ferrous site of distorted tetrahedral symmetry. The complex is highly covalent and cannot be explained by a purely ionic model.

Experimental Methods

Apoprotein free of acid-labile sulfur and iron was prepared by anaerobic trichloroacetic acid precipitation of putidaredoxin at room temperature (Tsibris *et al.*, 1968a). ^{57}Fe-enriched proteins were reconstituted from apoprotein by adding a sixfold molar excess of $^{57}FeCl_2$ and Na_2S or $(NH_4)_2Se$ (Tsibris *et al.*, 1968a,b). Considerable care was taken to avoid excessive exposure of the protein to oxygen, especially in the case of the selenium analog. The reconstituted proteins were purified on DEAE-cellulose columns, eluted with 0.5 M KCl buffer, and dialyzed at room temperature under anaerobic conditions. The dialysates were concentrated to 1–3 mM by ultrafiltration, applied to a Chelex-100 column, and eluted into the Mössbauer cell. The ^{57}Fe-putidaredoxin samples had biological activity and physical parameters identical with those of the native protein. Se-putidaredoxin samples showed biological activity and visible absorption and electron paramagnetic resonance (epr) spectra as described previously (Tsibris *et al.*, 1968b). The samples, typically about 20 mg of protein, were buffered with 50 mM Tris-chloride (pH 8.2). They were frozen in a nylon sample cell with a cross-sectional area of about 1 cm^2 and then transferred to the cryostat for measurement, or stored at 77°K.

The Mössbauer spectrometer was of the constant acceleration type. Data for positive and negative acceleration were stored separately in two halves of a multichannel analyzer and then folded. A 60-mCi source of ^{57}Co in copper was used which gave a minimum observable line width (FWHM) of 0.25 mm/sec. Using a Kr-filled proportional counter typical count rates in the 14.4-keV line were 20000 sec^{-1} with a peak area to background ratio of 5:1. The system was calibrated with a metallic iron absorber; all isomer shifts δ are listed relative to this standard.

The irradiation of the samples by the ^{57}Co source did not measurably change the biological activity of the protein.

A Janis variable-temperature cryostat was used for most of the measurements. The samples were inserted into the tail section from the top and the γ rays from the ^{57}Co(Cu) source passed horizontally through the sample *via* two pairs of mylar windows. The temperature could be stabilized anywhere from 1.7°K to room temperature.

A pair of coils were mounted around the tail section to produce a moderate parallel or transverse magnetic field at the sample. Due to vibrations in the tail section, samples measured in the cryostat typically had a minimum line width of 0.26 mm/sec.

A second cryostat with a split coil superconducting solenoid was used for measurements at 4.2°K in applied magnetic fields up to 50 kG. The coil was operated in the persistent mode. The field was calibrated with a Rawson-Lush rotating coil gaussmeter and its stability was monitored with an external Hall probe. A stray field of 2 kG at the source and vibrations in the cryostat led to some line broadening.

TABLE I: Data on Oxidized Putidaredoxin in Zero Field and in an Applied Magnetic Field, $H = 40.5 \pm 0.1$ kG.[a]

	Zero Field Data	Applied Field Data
Temperature (°K)	150	4.2
ΔE_Q (mm/sec)	0.595 (5)	+0.602 (5)
η		0.42 (2)
$\delta_{Fe\ metal}$ (mm/sec)	0.18 (1)	0.27 (2)
Line width (mm/sec)[b]	$\Gamma_1 = 0.294$ (3)	0.37 (6)
	$\Gamma_2 = 0.315$ (3)	
H_{int} (kG)		37.9 (2)
χ^2 of computer fit	0.77	0.99

[a] The numbers in parentheses represent the errors of the least significant digit. [b] Γ_2 is the line width of the higher energy peak; the greater line width in the applied field data is due to vibrations in the dewar system containing the superconducting solenoid.

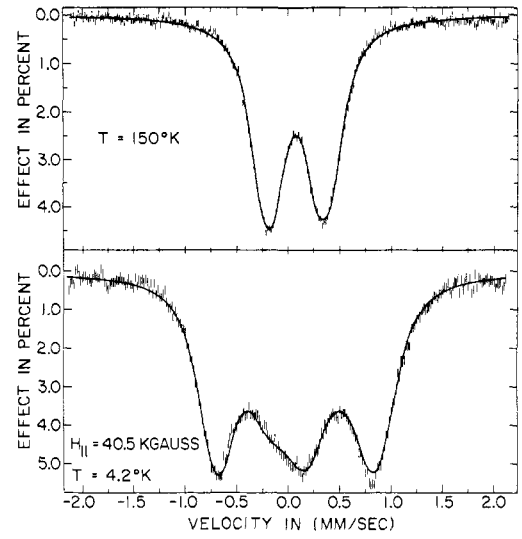

FIGURE 2: Mössbauer spectra of oxidized Se-putidaredoxin in zero field (upper curve) and in a magnetic field of 40.5 kG (lower curve). The zero-field spectrum is fitted with four Lorentzians equal in width and area corresponding to two nonequivalent sites. The two possible assignments of quadrupole pairs listed in Table II lead to indistinguishable fits for the high-field data; the solid line represents the fit for case 1.

Results

Oxidized Proteins. In a previous study of oxidized putidaredoxin (Cooke *et al.*, 1968), the Mössbauer spectra of the two iron atoms were found to be indistinguishable and characteristic of pure quadrupole interaction. In order to determine the sign of the quadrupole coupling constant and the value of the asymmetry parameter, we measured the spectra in a strong magnetic field. The results are shown in Figure 1; the upper curve represents the zero-field spectrum and the lower curve the spectrum observed in a field of 40.5 kG parallel to the direction of the γ rays.[1]

The eigenstates of a nucleus with spin I in the presence of quadrupole interaction and of an applied magnetic field $\mathbf{H}$ can be calculated from the Hamiltonian

$$\mathcal{H} = \frac{eQV_{zz}}{4I(2I-1)}[3I_z^2 - I(I+1) + \eta(I_x^2 - I_y^2)] - g_N\beta_N\mathbf{H}\cdot\mathbf{I} \quad (1)$$

Here Q is the nuclear quadrupole moment, V_{xx}, V_{yy}, and V_{zz} are the principal axis components of the quadrupole tensor, $\eta = (V_{xx} - V_{yy})/V_{zz}$ is the asymmetry parameter and $g_N\beta_N\mathbf{I}$ is the nuclear magnetic moment operator with components $\mathbf{I}_x$, $\mathbf{I}_y$, and $\mathbf{I}_z$. The quadrupole interaction vanishes for the nuclear ground state with spin $I = 1/2$, and since the excited state has spin $I = 3/2$ the quadrupole splitting observed in zero magnetic field is equal to

$$\Delta E_Q = 1/2\ eQV_{zz}\sqrt{1 + 1/3\eta^2}$$

To analyze the data a computer program was written which calculates Mössbauer spectra from the Hamiltonian, eq 1, for random orientation of the quadrupole tensor.[2] This program was then coupled to a least-squares-fitting routine which optimized the parameters V_{zz}, η, and H of eq 1, adjusting at the same time the isomer shift δ and the line width Γ. The results are given in Table I.

The Mössbauer parameters of the zero-field spectrum agree with the previously reported values[1] (Cooke *et al.*, 1968). A good fit to the high-field data could not be achieved unless the magnetic field H in eq 1 was reduced by $\Delta H \simeq 2.5$ kG below the value of the applied field.[3] Again the parameters for the two iron atoms are indistinguishable.

The zero-field spectrum of Se-putidaredoxin shows a similar pair of lines as native putidaredoxin, but the lines are considerably broader and of nonlorentzian shape (see Figure 2). Except for a second-order Doppler shift the Mössbauer spectrum does not change between 4.2°K and 200°K. In contrast to native putidaredoxin the spectrum cannot be fitted by two lorentzian lines. Excellent agreement with experiment is achieved, however, by fitting four Lorentzians with equal widths and intensities. We therefore conclude that Se-putidaredoxin has two different iron sites each giving rise to a separate quadrupole pair. Table II shows the two possible ways of pairing the four lines. For fitting the high-field data the quadrupole splittings and isomer shifts were taken from the zero-field spectra measured at 4.2°K and were treated as fixed parameters, while the asymmetry parameters, the magnetic fields and the line widths were allowed to be free. The

[1] The two lines of the zero-field spectrum in Figure 1 can be fitted by two Lorentzians of equal area but slightly different line width, $\Gamma_1 = 0.294 \pm 0.003$ mm/sec and $\Gamma_2 = 0.315 \pm 0.003$ mm/sec. The asymmetry can be explained as the result of a superposition of two slightly different doublets, one of which might be due to a small impurity. An unrestricted four-line fit did not converge to a meaningful result, however, and the possibility that the two irons of the enzyme have slightly different doublets cannot be ruled out from the data shown. For the analysis of the high-field data the detailed interpretation of the zero-field spectrum is irrelevant, since for the latter the experimental line width, $\Gamma = 0.37 \pm 0.06$ mm/sec, is considerably larger than Γ_1 or Γ_2. The line broadening in the high-field measurements is due to a stray field of 2 kG at the source and due to vibrations in the cryostat.

[2] In all calculations the recoilless fraction f is assumed to be isotropic, *i.e.*, Karyagin-Goldanskii effect (Karyagin, 1963; Goldanskii *et al.*, 1962) is not taken into account. The data show no evidence that this assumption is inadequate.

[3] To check for a possible decay of the magnetic field in the solenoid, the measurements were repeated monitoring the stability of the field with a Hall probe gaussmeter. At the beginning and at the end of the measurement the field was measured with a Rawson-Lush rotating coil gaussmeter and found to be $H = 40.5 \pm 0.1$ kG.

TABLE II: Data on Oxidized Se-Putidaredoxin in Zero Field and in an Applied Magnetic Field $H = 40.5 \pm 0.1$ kG.[a]

	Case 1		Case 2	
	Site 1	Site 2	Site 1	Site 2
ΔE_Q (mm/sec)	0.408 (5)	0.685 (5)	0.536 (5)	0.557 (5)
$\delta_{Fe\ metal}$ (mm/sec)	0.26 (1)	0.27 (1)	0.19 (1)	0.33 (1)
Γ (mm/sec)	0.30 (1)	0.30 (1)	0.30 (1)	0.30 (1)
Sign ΔE_Q	*b*	+	+	+
η	0.95 (3)	0.68 (3)	0.56 (3)	0.35 (3)
H_{int} (kG)	38.4 (3)	36.9 (3)	37.9 (3)	37.5 (3)
Γ (mm/sec)	0.38 (5)		0.33 (5)	
χ^2	1.15		1.13	

[a] The first three rows give the parameters as derived from a four line least-squares fit of the zero-field spectrum ($\chi^2 = 1.09$). Cases 1 and 2 refer to the two possibilities of pairing the four Lorentzians. The next rows give the additional information obtained from the high-field data. For the fits to the high-field spectra the absolute values of the quadrupole splittings and the difference in isomer shift δ for sites 1 and 2 were taken as found for the zero-field data and were treated as fixed parameters. The numbers in parentheses are the errors in the least significant digit. [b] For $\eta \approx 1$ sign ΔE_Q is meaningless since $V_{xx} \approx 0$ and $V_{yy} \approx -V_{zz}$.

results in Table II show that on the basis of these data no choice can be made between the two sets of parameters. Again the fields seen by the iron nuclei are smaller than the externally applied field.

To summarize, the spectra of oxidized putidaredoxin can be fitted with a single set of parameters, while Se-putidaredoxin requires two slightly different sets, *i.e.*, the two iron sites are not equivalent.

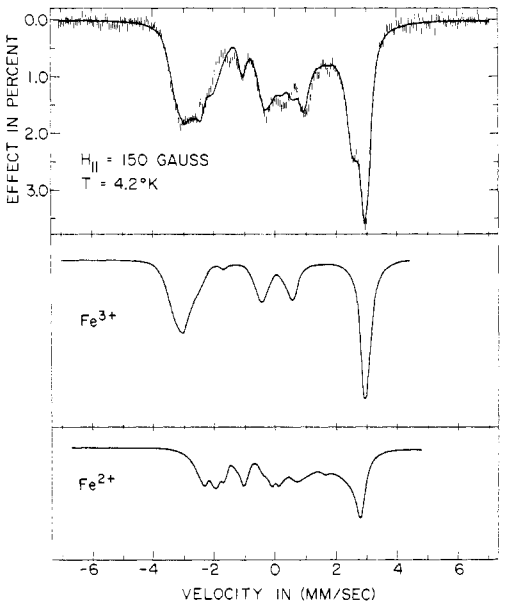

FIGURE 3: Mössbauer spectra of reduced putidaredoxin in a magnetic field of 150 G applied parallel to the γ rays. The lower curves show the decomposition of the simulated spectra into a spectrum (a) labeled Fe^{3+} and a spectrum (b) labeled Fe^{2+}. For the simulations in Figures 3–5 the center parts of the experimental spectra (±0.7 mm/sec) were ignored.

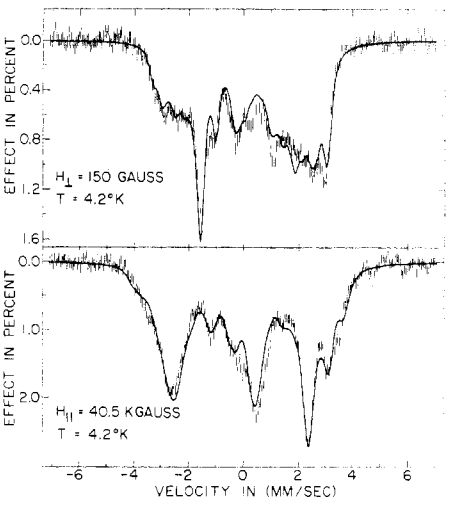

FIGURE 4: Mössbauer spectra of reduced putidaredoxin in a transverse field of 150 G and in a 40.5-kG parallel field. The same parameters, listed in Table III, were used to simulate the spectra in Figures 3 and 4.

Reduced Proteins. Mössbauer spectra for the reduced putidaredoxins taken at 4.2°K are shown in Figures 3–5. The spectra are very complicated and show only a few prominent absorption bands. A comparison of the data in Figures 3–5 shows that the spectra taken under comparable conditions for the sulfur and the selenium protein are quite similar. The large overall splitting and the strong dependence of the spectra on the direction of the weak, externally applied magnetic field are clear evidence of magnetic hyperfine interaction. At higher temperatures the magnetic interaction averages out due to faster electron spin relaxation, and the spectrum simplifies until at 200°K only four distinct lines can be seen (Figure 6). In the following, we will discuss the limiting cases of slow and fast relaxation only. It should be noted that all low-temperature spectra shown were taken in an external magnetic field. Zero-field spectra are radically different.[4]

Before discussing the various spectra a remark is necessary about the reproducibility of the data. Comparison of spectra taken on different preparations shows small variations in the center part, -0.7 mm/sec $< v < 0.7$ mm/sec. Since the oxidized samples usually gave little or no evidence for any impurity, we first attributed it to the dithionite used for reduction. However, we observed similar effects in samples that were reduced biologically with DPNH and putidaredoxin oxireductase. Apparently the variations in absorption are due to the presence of small amounts (<4%) of nonspecifically bound iron, not readily detectable by Mössbauer measurements in the oxidized state. This explanation is compatible with the trace paramagnetism observed in oxidized putidaredoxin by magnetic susceptibility measurements (Moleski *et al.*, 1970) (impurity of <2–3%, if attributed to high-spin ferric iron).

No changes in the Mössbauer spectra are observed in reduced samples of both enzymes when the temperature is raised to about 80°K. At still higher temperature the spin-

[4] The previously published Mössbauer spectra of reduced putidaredoxin are not reproducible since the magnetic field at the sample was not defined. The spectra as well as the attempts to interpret them should therefore be ignored (Cooke *et al.*, 1968).

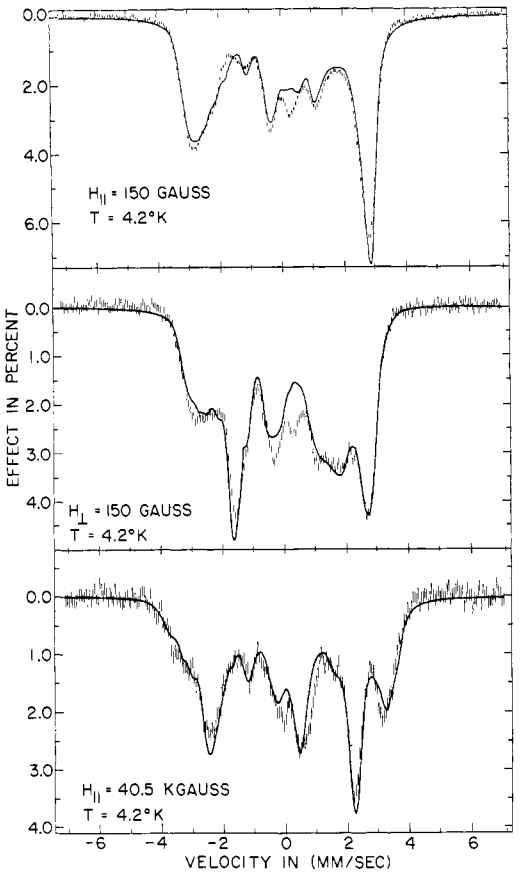

FIGURE 5: Mössbauer spectra of reduced Se-putidaredoxin taken at 4.2°K in moderate and strong magnetic fields. Upper spectrum: 150 G parallel to the γ rays. Middle: 150-G perpendicular field. Lower spectrum: 40.5 kG parallel to the γ rays. The simulated curves represent the parameters in Table III.

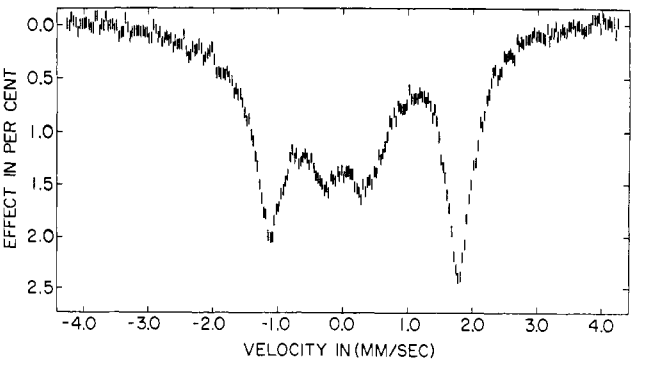

FIGURE 6: Spectrum of reduced Se-putidaredoxin taken at 195°K in a moderate magnetic field parallel to the γ rays.

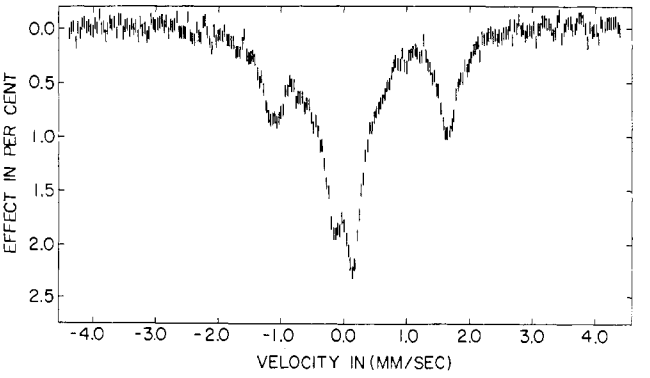

FIGURE 7: Mössbauer spectrum of a lyophilized sample of reduced putidaredoxin taken at room temperature. The strong absorption in the center part is due to denatured material.

lattice relaxation time becomes sufficiently short that the magnetic interaction partly averages out. But even near room temperature, some residual magnetic interaction is left. Putidaredoxin differs in this respect from the green plant ferredoxins which have comparable relaxation rates already at 80°K (Johnson *et al.*, 1968; Dunham *et al.*, 1971). Figure 6 shows the spectrum of reduced Se-putidaredoxin taken at 195°K. Four distinct lines appear, that can be interpreted as two doublets, each of which can be associated with one iron atom. The inner pair of lines resembles the spectrum of the oxidized protein and is likely to arise from an iron site unchanged by the reduction process. The values for the quadrupole splitting ΔE_Q and the isomer shift δ agree with those found for the oxidized sample within the accuracy with which these parameters can be evaluated in the presence of residual magnetic interaction. The quadrupole splitting of the outer pair is $\Delta E_Q = 2.92$ mm/sec, and the isomer shift is $\delta = 0.55$ mm/sec with respect to metallic iron. Both values strongly suggest that the outer doublet arises from an iron atom in a high-spin ferrous state. The isomer shift is considerably smaller than the one found in ionic ferrous complexes, but this can reasonably be attributed to the effect of covalency. The small difference of 0.31 mm/sec in the isomer shifts is comparable to the change observed in rubredoxin. Rubredoxin has four sulfurs tetrahedrally coordinated to iron, and shows a difference in isomer shift of 0.2 mm/sec between the oxidized ferric state ($S = 5/2$) and the reduced, ferrous ($S = 2$) state (Phillips *et al.*, 1970).

For putidaredoxin the spin-lattice relaxation time is longer than for the selenium analog so that even at 250°K the magnetic interaction is not averaged out sufficiently to determine the quadrupole splittings for a sample kept in a frozen solution. Figure 7 shows the Mössbauer spectrum of lyophilized reduced material at room temperature. A quadrupole splitting of about 2.8 mm/sec is found for the ferrous site.[5]

It now remains to be seen whether the low-temperature data (Figures 3–5) can also be explained as a superposition of two spectra, one of them due to the ferric iron and the other due to the ferrous. The relation between the physical parameters of the individual atoms and the complex as a whole will be treated in the Discussion section. Here we start from the empirical fact that the paramagnetic complex has an electron spin of $S = 1/2$ which interacts with the two iron nuclei of spin I_a and I_b and with the applied magnetic field $\mathbf{H}$. Such a system can be described by the Hamiltonian

$$\mathcal{H}(S = 1/2) = \beta_e \mathbf{H}\tilde{g}\mathbf{S} + \mathbf{S}\tilde{A}_a\mathbf{I}_a + \mathbf{S}\tilde{A}_b\mathbf{I}_b + \mathcal{H}_N(a) + \mathcal{H}_N(b) \quad (2)$$

Here β_e is the Bohr magneton, $\tilde{g}$ the g tensor of the paramag-

[5] The large intensity of the center doublet in Figure 7 suggests a partly oxidized sample. However, the optical spectrum taken when the sample was anaerobically redissolved gave no indication of any oxidized material. After reoxidation, the Mössbauer spectrum showed some anomalous absorption to the right of the higher energy peak. Passing the sample through a Chelex-100 column restored the original symmetric spectrum. Thus it appears that an appreciable amount of the protein denatured upon lyophilization.

netic center, $\tilde{A}_a$ and $\tilde{A}_b$ are the hyperfine tensors and $\mathcal{H}_N(a)$, and $\mathcal{H}_N(b)$ are the nuclear Hamiltonians, defined by eq 1, for the nuclei (a) and (b), respectively. A computer program was written that calculates Mössbauer spectra for a system described by eq 2 in the thin absorber limit.[2]

The program has the following features and limitations.[6] (1) An infinite electron spin relaxation time is assumed. (2) The g tensor, the hyperfine tensors $\tilde{A}_a$ and $\tilde{A}_b$, and the quadrupole tensors are allowed to have arbitrary orientations. (3) A sufficiently strong applied field H is assumed, *e.g.*, $H \gg 15$ G, such that the Zeeman term in eq 2 is much larger than all the other terms. Condition 3 simplifies the calculation considerably. A coordinate frame can be found in which the Zeeman term is diagonal, $\mathcal{H}_{Zeeman} = \beta_e g' H S_z'$. Neglecting off-diagonal terms of $\mathbf{S}$ in the hyperfine term ($\mathbf{S}_x'\mathbf{I}_x'$, $\mathbf{S}_y'\mathbf{I}_z'$, etc.), the remainder of the Hamiltonian depends on the nuclear spins only. It can be separated into two parts, depending on $\mathbf{I}_a$ and $\mathbf{I}_b$, respectively. Each part is then diagonalized separately to determine the nuclear eigenstates and eigenvalues. The eigenstates are used to calculate the intensities of the Mössbauer spectrum. Finally a proper average over all molecular orientations is taken.

The effect of the applied magnetic field is twofold. (i) It polarizes the spin doublet, $S = 1/2$, giving rise to two states with opposite spins, $S_z' = \pm 1/2$. The electron spin in turn determines *via* the A tensor the direction of the internal magnetic field at the nucleus. In moderate fields the two states, $S_z' = \pm 1/2$, produce Mössbauer spectra which cannot be distinguished. Since the g tensor in putidaredoxin is nearly isotropic, the quantization axis of the electron spin is practically parallel to the magnetic field. This explains the drastic change in the Mössbauer spectrum if the direction of the field is changed from parallel to perpendicular with respect to the γ rays observed. (ii) In strong magnetic fields the splitting of the electronic ground state, $E_{1/2} - E_{-1/2} = \beta_e g' H$, is comparable to kT and the populations of the two spin states $S_z' = \pm 1/2$ are different. The external field either adds to the internal field or opposes it, and for each site (a) and (b) the total Mössbauer spectrum then is a sum of two different spectra, one for each spin state, weighted with the appropriate Boltzmann factor.

The direction of the internal field, $\mathbf{H}_{int} = -\tilde{A}\langle\mathbf{S}\rangle/(\beta_N g_N)$, relative to the applied field can thus be determined from the spectrum, and since the spin direction, $S_z' = \pm 1/2$, can be obtained from the size of the Boltzmann factor, it is possible to determine the sign of the A tensor from strong-field Mössbauer data. As will be discussed later, the internal field is parallel to $\langle\mathbf{S}\rangle$ at the a site and antiparallel at the b site.

To specify a Mössbauer spectrum completely, the following parameters are required, g_x, g_y, g_z, A_x, A_y, A_z, V_{zz}, η, H, the isomer shift δ, the line width Γ, and the six Euler angles defining the orientation of the principal axes of the A tensor and the quadrupole tensor with respect to the g tensor. Fortunately some of these parameters are known and fixed values can be assumed for others since they hardly affect the spectrum.

In view of the difficulties in achieving unambiguous results when many parameters are adjusted, it seems appropriate to discuss in some detail the procedure by which our results were obtained. (1) The g values are known from electron spin resonance (esr) measurements (Orme-Johnson *et al.*, 1968). (2) Electron nuclear double resonance (endor) measurements (Fritz *et al.*, 1971, and R. H. Sands, 1970, private communication) provide the absolute values for the components of the A tensor of the ferric iron and indicate that its principal axes are parallel to those of the g tensor. (3) For the ferrous site, there is an endor resonance at 35 ± 1.5 MHz (Fritz *et al.*, 1971). (4) The signs for the A values for both iron sites can be extracted from the low temperature Mössbauer spectra taken in high magnetic field. (5) The high-temperature Mössbauer data give the isomer shifts and the quadrupole splittings for both sites. These parameters can be used as good starting values for the low-temperature data. (6) Since the g tensor is nearly isotropic, the Mössbauer spectrum is insensitive to a rotation of $\tilde{A}$ with respect to $\tilde{g}$, so that angles between $\tilde{g}$ and $\tilde{A}$ can be arbitrarily set equal to zero.

The program first was written for the IBM 360 system, but later adapted to a CDC 1604 computer with CRT display. This approach allowed direct visual comparison of the simulated spectra with the experimental data and a systematic search could be done more efficiently. In this way hundreds of spectra were calculated, put on display and photographed. The data taken in moderate parallel magnetic field were analyzed first, since only two angles are required for a "powder" integration.[7] After a series of simulations the improved parameters were cross-checked by computing spectra for perpendicular and high magnetic fields. Whenever a set of parameters was found describing the spectra fairly well, the simulation program was coupled to a least-squares-fitting program.[8] Although it is unlikely that the fitting routine converges to a unique solution, this procedure allowed to find stable minima for some of the parameters. The center parts (± 0.7 mm/sec) of the spectra were excluded from the fitting because of the lack of reproducibility in this region mentioned above.

It is appealing to assume that the samples contain variable amounts of an impurity with a Mössbauer spectrum that cannot be distinguished from the spectrum of the oxidized protein. Adding a pair of lines at the position where the absorption occurs in the oxidized sample, in fact, improves the fit visually, but presently we have no direct evidence that this procedure is justified.

When the initial parameters for the ferrous site were varied within reasonable bounds, the program only converged to a better solution if the largest component of the A_b tensor was not greater than 34 MHz. The endor resonance at 35 ± 1.5 MHz measured along g_z must therefore be a principal axis value (*i.e.*, A_z when referred to the g frame) or close to it. This determines two of the three angles describing the relative orientation of $\tilde{A}_b$ with respect to $\tilde{g}$.

The results of the simulations are represented by the solid lines in Figures 3–5, and the parameters obtained are listed in Table III. The quoted errors are estimates based on visual inspection of many simulated spectra. The parameters in parenthesis could not be determined reliably. Keeping in mind that the center parts of the spectra were excluded from the simulation procedure, it can be seen that the parameters fit the data fairly well. Slight spectral variations observed in different preparations do not justify a further extensive search for improvement of the parameters.

The results can be summarized as follows. For the ferric iron the only adjustable parameters are the orientation of the quadrupole tensor and the asymmetry parameter. Neither one can be determined accurately since the magnetic splitting dominates the quadrupole interaction.

[6] A detailed description of the program is in preparation.

[7] A 10 by 10 integration takes 3 sec on the IBM 360 system and about 50 sec on the CDC 1604.

[8] The least-squares-fitting program was written by Dr. J. L. Groves.

TABLE III: Low-Temperature Mössbauer Parameters for the Reduced Putidaredoxin Samples.[a]

	Native Putidaredoxin		Se–Putidaredoxin	
	Site a	Site b	Site a	Site b
g_x	1.94		1.93	
g_y	1.94		1.98	
g_z	2.01		2.04	
A_x (MHz)	−56 (+1, −3)[c]	14 (+3, −2)	−52.4 (+1, −3)[c]	14 (+4, −2)
A_y (MHz)	−50 ± 1.5[c]	21 ± 4	−48.2 ± 1.5[c]	17 ± 4
A_z (MHz)	−43 (−1, +2)[c]	35 ± 1.5[c]	−40.5 (−1, +2)[c]	34 ± 2[c]
ΔE_Q (mm/sec)	+0.6 ± 0.1	−2.7 ± 0.1	+0.55 ± 0.1	−2.9 ± 0.1
$eQV_{zz}/2$ (mm/sec)	(+0.57)	−1.35	(+0.53)	−1.45
η	(0.5)	−3[d]	(0.5)	−3
$\delta_a - \delta_b$ (mm/sec)	−0.31 ± 0.03		−0.32 ± 0.03	
Γ[b]	0.31 ± 0.02		0.34 ± 0.02	

[a] All parameters are referred to the principal axis system of the g tensor. [b] Width (FWHM) of the assumed lorentzian lines. No attempt was made to calculate the spectra for both sites with different line widths. [c] Absolute values were obtained by endor measurements (Fritz *et al.*, 1971; R. H. Sands, private communication. [d] The quadrupole tensor is referred to the g frame; $\eta = -3$ means that the quadrupole tensor has axial symmetry around the x axis.

The ferrous A tensor has one large component and two smaller ones of about equal magnitude, all components having a positive sign. Though the Mössbauer spectra are insensitive to the relative orientation of $\tilde{g}$ and $\tilde{A}_b$ the systematic search through parameter space enables us to identify the large component of $\tilde{A}_b$ as a principal axis value and connect it with the endor resonance found at 35 ± 1.5 MHz. Referred to the principal axis of the g tensor, this component is A_z. The largest component of the quadrupole tensor is positive and perpendicular to A_z within ±15° of the x–y plane. The best results were obtained when the quadrupole tensor had axial symmetry about its largest component, *i.e.*, $\eta = 0$ in the principal axis frame of the quadrupole tensor. When the parameters for $\tilde{A}_b$ and η are fixed and the quadrupole tensor is rotated around the z axis, it is found that the principal axes of both tensors nearly coincide and that the largest component of the quadrupole tensor is V_{xx} (in the g frame). These results apply to both the S- and the Se-protein.

Discussion

The spin-coupling model of Gibson *et al.* (Gibson *et al.*, 1966; Thornley *et al.*, 1966) provides a natural explanation for most of the results just presented. The model assumes an exchange interaction between the spins S_a and S_b of the two iron atoms which, in its simplest form, can be written as: $\mathcal{H}_{ex} = J\mathbf{S}_a \cdot \mathbf{S}_b$, $J > 0$. The Hamiltonian $\mathcal{H}_{ex}$ has eigenstates of spin S, $\mathbf{S} = \mathbf{S}_a + \mathbf{S}_b$, $S = |S_a - S_b|, \ldots, S_a + S_b$, and the energy of a state with spin S is given by $E(S) = (J/2)S(S+1)$ + constant. According to Gibson *et al.*, the diamagnetism of the oxidized 2Fe–2S proteins results from the coupling of two ferric ions of spin $S_a = S_b = 5/2$, to a ground state of spin $S = 0$. The first excited state with spin $S = 1$ occurs at an energy J above the ground state. From magnetic susceptibility measurements on oxidized putidaredoxin J/k, where k is the Boltzmann constant, is conservatively estimated to be larger than 60°K (Moleski *et al.*, 1970). Similar limits on J apply for the reduced protein, in which a ferric ion of spin $S_a = 5/2$ is paired with a ferrous ion of spin $S_b = 2$ to form a ground state of spin $S = 1/2$. The details of the exchange interaction remain hypothetical as long as the structure of the iron complex is not known.

Each of the two iron atoms a and b is described by its own Hamiltonian of the form

$$\mathcal{H}_k = \beta\mathbf{H}\tilde{g}_k\mathbf{S}_k + \mathbf{S}_k\tilde{a}_k\mathbf{I}_k + \mathcal{H}_N(k),\ k = a,b \qquad (3)$$

Here $\tilde{g}_a$, $\tilde{g}_b$ and $\tilde{a}_a$, $\tilde{a}_b$ are the individual g tensors and hyperfine tensors, respectively, and $\mathcal{H}_N$ is the nuclear Hamiltonian defined in eq 1.

The total Hamiltonian of the system is the sum of $\mathcal{H}_{ex}$, $\mathcal{H}_a$, and $\mathcal{H}_b$. Since J is very large compared to $\mathcal{H}_a$, $\mathcal{H}_b$, and kT, we can define an effective Hamiltonian for the ground state of $\mathcal{H}_{ex}$, *i.e.*, for the doublet, $S = 1/2$. This effective Hamiltonian is identical with eq 2. We now obtain the following relation between the tensors of the individual ions, $\tilde{g}_a$, $\tilde{g}_b$, $\tilde{a}_a$, and $\tilde{a}_b$, and the tensors $\tilde{g}$ and $\tilde{A}_a$, $\tilde{A}_b$ in the coupled system (Gibson *et al.*, 1966; Thornley *et al.*, 1966)

$$\tilde{g} = \frac{7}{3}\tilde{g}_a - \frac{4}{3}\tilde{g}_b;\ \tilde{a}_a = \frac{3}{7}\tilde{A}_a,\ \tilde{a}_b = -\frac{3}{4}\tilde{A}_b \qquad (4)$$

Here it was assumed that the individual g and A tensors all have the same principal axis system. Note that A_b has the opposite sign of a_b because of the antiferromagnetic coupling.

The A tensor is in general a sum of three contributions referred to as orbital, dipolar, and contact term. The last term is isotropic in contrast to the first two, and it always dominates in high-spin compounds. For a purely ionic high-spin state it equals −30 MHz (Locher and Geschwind, 1965), which is equivalent to an internal magnetic field of 110 kG/spin 1/2, $H_{int}/S = -A/(\beta_N g_N)$. If we interpret our experimental results (Table III) in terms of the model just outlined, we arrive at the following conclusions. (1) The model properly accounts for the direction of the internal field at nucleus b, *i.e.*, the field is parallel to the spin $S_b = 2$ ($a_b < 0$) as is should be in view of the dominance of the contact term, but it is antiparallel to the resultant spin $S = 1/2$ ($A_b > 0$) because of the antiferromagnetic coupling. (2) The average values, $\langle a_a \rangle = -21$ MHz, and $\langle a_b \rangle = -17.5$ MHz, of the A tensors of the a and b sites of putidaredoxin are considerably smaller than the value

$A = -30$ MHz expected for an ionic iron compound. This implies that the 3d electrons of both irons are highly delocalized. The internal field, $H_{int} = -A\langle S\rangle/\beta_N g_N = -375$ kG observed in ferric rubredoxin (Phillips *et al.*, 1970) is equivalent to a value of $A = -21$ MHz which is identical with the value found for site a. (3) The A tensor of the a site has an anisotropy of $\pm 10\%$ which is about ten times larger than the values commonly observed in high-spin ferric compounds. So large an anisotropy cannot be explained in the usual ligand field approximation. (4) The interpretation of site b in the reduced protein as ferrous high spin is consistent with the observed isomer shift, the quadrupole coupling and the hyperfine tensor. The anisotropy of $\tilde{a}_b$ is not unusual since orbital and spin dipolar terms contribute. The relatively small size of $\langle a_b\rangle$ and of the isomer shift again indicate strong delocalization of the 3d electrons. An interpretation of V_{ij} and $\tilde{a}_b$ in terms of standard 3d orbitals is therefore at best an approximation. (5) Once we have interpreted the a site in reduced putidaredoxin as a ferric high-spin iron, there is little doubt that both irons in the oxidized protein are high-spin ferric as well, since they have the same isomer shifts and quadrupole splittings.

In summary the spin-coupling model, eq 2-4, provides a consistent explanation of our experimental results. The same conclusion was reached for the plant ferredoxins by other groups (Dunham *et al.*, 1971; Johnson *et al.*, 1971; Rao *et al.*, 1971).

We next turn to a discussion of the spatial configuration of the 2Fe–2S complex. Gibson (Gibson *et al.*, 1966) and others (Brintzinger *et al.*, 1966) proposed a tetrahedral arrangement of sulfur ligands around the two iron atoms. In tetrahedral symmetry the ligand field is relatively weak and leads to a high-spin configuration. The unusual g values of the reduced protein can be explained if the ferrous site is assumed to have distorted tetrahedral symmetry. It is tempting to assume that each of the two acid-labile sulfur atoms acts as a bridging ligand between the two iron atoms thus allowing for Fe–S–Fe superexchange. If in addition four of the four to six cysteins that are invariably found in the 2Fe–2S proteins (Buchanan and Arnon, 1970; Hall *et al.*, 1971; Tsai *et al.*, 1971) bind to the two iron atoms (Poe *et al.*, 1971) we arrive at a simple model of an exchange coupled pair of tetrahedrally coordinated iron atoms (Gibson *et al.*, 1966; Cooke *et al.*, 1968; Dunham *et al.*, 1971; Johnson *et al.*, 1971; Rao *et al.*, 1971).

The strongest evidence for distorted tetrahedral symmetry at the ferrous iron comes from Mössbauer spectroscopy on green plant ferredoxins (Dunham *et al.*, 1971). The b sites of both spinach and parsley ferredoxin have a negative quadrupole interaction of axial symmetry about the z axis, where the z axis is defined by the largest component of the g tensor. Such a quadrupole tensor is uniquely characteristic of an electronic ground state of symmetry d_{z^2}. Moreover the temperature dependence of the quadrupole splitting suggests the existence of a first excited state of symmetry $d_{x^2-y^2}$ at an energy of about 500 cm^{-1} (Dunham *et al.*, 1971). Both facts indicate a b site of distorted tetrahedral symmetry in spinach and parsley ferredoxin.

For the putidaredoxins the situation is ambiguous. In the reduced protein the b site also has a quadrupole tensor of axial symmetry, but the axis is along the x direction of the g tensor, and the principal value is positive.[9] If we define a rotated coordinate system $\bar{x}$, $\bar{y}$, $\bar{z}$, by the substitution $x \rightarrow \bar{z}$, $y \rightarrow \bar{x}$, $z \rightarrow \bar{y}$, the quadrupole tensors in the rotated frame, $\Delta E_Q = +2.7$ mm/sec, $\eta = 0$ for putidaredoxin, and $\Delta E_Q = +2.9$ mm/sec, $\eta = 0$ for Se-putidaredoxin, are consistent with either a $d_{\bar{x}^2-\bar{y}^2}$ or a $d_{\bar{x}\bar{y}}$ orbital. Octahedral, square planar or square pyramidal symmetries are all compatible with a ground state of $d_{\bar{x}\bar{y}}$ symmetry, but these interpretations require unusually large splittings of the d orbitals by rhombic distortion to account for the observed g values. A $d_{\bar{x}^2-\bar{y}^2}$ orbital, however, is compatible with distorted tetrahedral symmetry, and we prefer this interpretation for the following reasons. (i) The b site of parsley and spinach ferredoxin was shown to have distorted tetrahedral symmetry and, in view of the great similarities in the properties of the active centers of all 2Fe–2S proteins, it is unlikely that the structure of the ferrous site in putidaredoxin is substantially different; (ii) in the ligand field model adopted here the g tensor of putidaredoxin can be explained with reasonable values for the splitting of the 3d orbitals.

For a $d_{\bar{x}^2-\bar{y}^2}$ orbital at the ferrous site we obtain

$$g_{\bar{x}} = \frac{7}{3}g_{a\bar{x}} - \frac{4}{3}g_{b\bar{z}} = g_e + \frac{7}{3}\Delta g_{a\bar{x}} - \frac{32}{3}\frac{\lambda}{\Delta_{\bar{x}\bar{y}}}$$

$$g_{\bar{y}} = \frac{7}{3}g_{a\bar{y}} - \frac{4}{3}g_{b\bar{x}} = g_e + \frac{7}{3}\Delta g_{a\bar{y}} - \frac{8}{3}\frac{\lambda}{\Delta_{\bar{y}\bar{z}}}$$

$$g_{\bar{z}} = \frac{7}{3}g_{a\bar{z}} - \frac{4}{3}g_{b\bar{y}} = g_e + \frac{7}{3}\Delta g_{a\bar{z}} - \frac{8}{3}\frac{\lambda}{\Delta_{\bar{x}\bar{z}}}$$

Here we define $\Delta g_{a\bar{x}} = g_{a\bar{x}} - g_e$, etc., where g_e is the free electron g value, $\lambda \approx 80$ cm^{-1} is the spin orbit coupling constant for the ferrous ion, and $\Delta_{\bar{x}\bar{y}}$, $\Delta_{\bar{y}\bar{z}}$, and $\Delta_{\bar{x}\bar{z}}$ are the energy separations of the $d_{\bar{x}\bar{y}}$, $d_{\bar{y}\bar{z}}$ and $d_{\bar{x}\bar{z}}$ orbitals from the ground state $d_{\bar{x}^2-\bar{y}^2}$. In a distorted tetrahedral environment we expect the Δ's to be of the order of 3000–7000 cm^{-1} (Slack *et al.*, 1966; Edwards *et al.*, 1967; Eaton and Lovenberg, 1970).

Within this range of orbital energies an anisotropy of $\Delta g_a/g_e < 2\%$ can fully account for the observed g values. Such anisotropies have been reported for Fe^{3+} in tetrahedral FeS_2Se_2 clusters (Schneider *et al.*, 1968) ($g_x = 2.049(10)$, $g_y = 2.020(10)$, $g_z = 2.054(3)$, and $\langle g\rangle = 2.041$). For putidaredoxin we expect to find an anisotropy in g that is at least as large, in particular since the A_b tensor indicates sizable deviations from tetrahedral symmetry.

To summarize, the Mössbauer data of the putidaredoxins do not allow an unambiguous interpretation of the parameters in terms of symmetry of the active site. Within the crystal field approximation, however, the data are compatible with a ferrous site of distorted tetrahedral symmetry. With this interpretation the structures of the active sites of green plant ferredoxins and of putidaredoxin may be essentially the same.

Acknowledgment

We thank Dr. R. H. Sands, Biophysics Research Division, University of Michigan, Ann Arbor, for valuable discussions on his endor results prior to publication, and we are grateful to M. J. Namtvedt for the preparation of the numerous samples.

References

Brintzinger, H., Palmer, G., and Sands, R. H. (1966), *Proc. Nat. Acad. Sci. U. S. 55*, 397.

[9] We tried unsuccessfully to simulate the spectra of reduced putidaredoxin with an axially symmetric quadrupole tensor of negative principal value at the b site as it was found in spinach and parsley ferredoxin (Dunham *et al.*, 1971).

Buchanan, B. B., and Arnon, D. I. (1970), *Advan. Enzymol. 33*, 119.

Cooke, R., Tsibris, J. C. M., Debrunner, P. G., Tsai, R., Gunsalus, I. C., and Frauenfelder, H. (1968), *Proc. Nat. Acad. Sci. U. S. 59*, 1045.

Cushman, D. W., Tsai, R. L., and Gunsalus, I. C. (1967), *Biochem. Biophys. Res. Commun. 26*, 577.

Der Vartanian, D. W., Orme-Johnson, W. H., Hansen, R. E., and Beinert, H. (1967), *Biochem. Biophys. Res. Commun. 26*, 569.

Dunham, W. R., Bearden, A., Salmeen, I., Fee, J., Petering, D., Sands, R. H., and Orme-Johnson, W. H. (1971), *Biochim. Biophys. Acta 253*, 134.

Eaton, W. E., and Lovenberg, W. (1970), *J. Amer. Chem. Soc. 48*, 7195.

Edwards, P. R., Johnson, C. E., and Williams, R. J. P. (1967), *J. Chem. Phys. 47*, 2074.

Fritz, J., Anderson, R., Fee, J., Petering, D., Palmer, G., Sands, R. H., Tsibris, J. C. M., Gunsalus, I. C., Orme-Johnson, W. H., and Beinert, H. (1971), *Biochim. Biophys. Acta 253*, 110.

Gibson, J. F., Hall, D. O., Thornley, J. H. M., and Whatley, F. R. (1966), *Proc. Nat. Acad. Sci. U. S. 56*, 987.

Goldanskii, V. I., Gorodinskii, L. M., Makarov, E. F., Suzdalev, I. P., Khrapov, V. V. (1962), *Dokl. Adad. Nauk SSSR 147*, 127.

Gunsalus, I. C. (1968), *Hoppe-Seylers Z. Physiol. Chem. 349*, 1610.

Hall, D. O., Cammack, R., and Rao, K. K. (1971), *Nature (London) 233*, 136.

Hall, D. O., and Evans, M. C. W. (1969), *Nature (London) 223*, 1342.

Herriott, J. R., Sieker, L. C., Jensen, L. H., and Lovenberg, W. (1970), *J. Mol. Biol. 50*, 391.

Johnson, C. E., Bray, R. C., Cammack, R., and Hall, D. O. (1969), *Proc. Nat. Acad. Sci. U. S. 63*, 1234.

Johnson, C. E., Cammack, R., Rao, K. K., and Hall, D. O. (1971), *Biochem. Biophys. Res. Commun. 43*, 564.

Johnson, C. E., Elstner, E., Gibson, J. F., Benfield, G., Evans, M. C. W., and Hall, D. O. (1968), *Nature (London) 220*, 1291.

Johnson, C. E., and Hall, D. O. (1968), *Nature (London) 217*, 446.

Karyagin, S. V. (1963), *Dokl. Adad. Nauk SSSR 148*, 1102.

Kraut, J., Strahs, G., and Freer, S. T. (1968), *in* Structural Chemistry and Molecular Biology, Rich, A., and Davidson, N., Ed., San Francisco, Calif., W. H. Freeman, p 55.

Locher, P. R., and Geschwind, S. (1965), *Phys. Rev. 139*, A991.

Moleski, C., Moss, T. H., Orme-Johnson, W. H., and Tsibris, J. C. M. (1970), *Biochim. Biophys. Acta 214*, 584.

Orme-Johnson, W. H., Hansen, R. E., Beinert, H., Tsibris, J. C. M., Bartholmaus, R. C., and Gunsalus, I. C. (1968), *Proc. Nat. Acad. Sci. U. S. 60*, 368.

Palmer, G., Brintzinger, H., and Estabrook, R. W. (1967), *Biochemistry 6*, 1658.

Palmer, G., and Sands, R. H. (1966), *J. Biol. Chem. 241*, 253.

Phillips, W. D., Poe, M., Weiher, J. F., McDonald, C. C., and Lovenberg, W. (1970), *Nature (London) 227*, 574.

Poe, M., Phillips, W. D., Glickson, J. C., McDonald, C. C., and San Pietro, A. (1971), *Proc. Nat. Acad. Sci. U. S. 68*, 68.

Rao, K. K., Cammack, R., Hall, D. O., and Johnson, C. E. (1971), *Biochem. J. 122*, 257.

Schneider, Y., Dischler, B., and Räuber, A. (1968), *J. Phys. Chem. Solids 29*, 451.

Slack, G. A., Ham, F. S., and Chrenko, R. M. (1966), *Phys. Rev. 152*, 376.

Thornley, J. H. M., Gibson, F. F., Whatley, F. R., and Hall, D. O. (1966), *Biochem. Biophys. Res. Commun. 24*, 877.

Tsai, R. L., Dus, K., and Gunsalus, I. C. (1971), *Biochem. Biophys. Res. Commun. 45*, 1300.

Tsibris, J. C. M., Namtvedt, M. J., and Gunsalus, I. C. (1968b), *Biochem. Biophys. Res. Commun. 30*, 323.

Tsibris, J. C. M., Tsai, R. L., Gunsalus, I. C., Orme-Johnson, W. H., Hansen, R. E., and Beinert, H. (1968a), *Proc. Nat. Acad. Sci. U. S. 59*, 959.

Tsibris, J. C. M., and Woody, R. W. (1970), *Coordin. Chem. Rev. 5*, 417.